www.ietdl.org

Published in IET Radar, Sonar and Navigation
Received on 15th December 2011
Revised on 19th February 2012
doi: 10.1049/iet-rsn.2011.0372

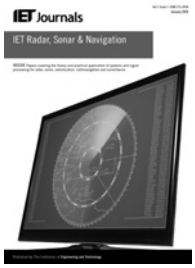


ISSN 1751-8784

# New waveform for magnetron marine radar – experimental results

*N. Levanon*[1] *E. Ben-Yaacov*[2] *D. Quartler*[1]

[1]*Department of EE-Systems, Tel-Aviv University, Tel-Aviv, Israel*
[2]*Elisra Ltd, Bnei-Brak, Israel*
*E-mail: nadav@eng.tau.ac.il*

**Abstract:** The unambiguous range of a pulse-radar is related to the pulse repetition interval (PRI). Most magnetron-based marine radars adjust the PRI according to the maximum displayed range. They correspondingly adjust the pulse-width (PW) to keep the ratio PW/PRI nearly constant. The extreme settings can be described as 'short pulse, short PRI' (SPSP) for short distances and 'long pulse, long PRI' (LPLP) for long distances. Such settings keep the transmitter's duty cycle and the energy-on-target, relatively constant. Penalties of long PW are large clutter area illumination and poor range resolution. Maintaining a short pulse is important in magnetron-based radar, because a magnetron does not lend itself to pulse compression. The study presents a method that allows operating in the SPSP mode for long distances as well. Both theory and experimental results are presented.

## 1 Introduction

Most low-cost civil marine radars are magnetron based, hence non-coherent [1]. Lacking the option of phase or frequency modulation, they cannot perform pulse-compression and the range resolution is determined by the pulse-width $t_p$. At short-range setting it is customary to use narrow pulses, short PRI and fast antenna rotation speed. At long-range setting, in order to extend the unambiguous range, the pulse repetition interval (PRI) is increased. The energy on target, related to the transmitter duty cycle, is maintained (approximately) by increasing the pulse width (PW). The energy on target is further increased by increasing the time-on-target (TOT) through lowering the antenna rotation speed. The relevant parameters from Furuno 1623 radar are listed in Table 1.

Two penalties come with increased PW: poorer range resolution and stronger clutter. It would therefore be advantageous if the short-pulse short-PRI (SPSP) mode could be maintained in the long-range settings. Towards that end, a periodic PRI-coded waveform was proposed in [2]. The present paper describes experimental results with such waveforms.

## 2 Waveforms

The periodic PRI codes start from binary sequences that exhibit ideal periodic autocorrelation, or ideal periodic cross-correlation with a slightly different reference sequence. Two codes were used in the field trials. One was based on Barker 4, which is the only known binary sequence with ideal periodic autocorrelation. The second was based on Ipatov 5 code [3]. Binary codes use two values $\{+1, -1\}$, but a magnetron cannot be polarity modulated; it can only be on–off keyed. So the Barker 4 or Ipatov 5 are Manchester coded: $+1$ is converted to $\{0, 1\}$ and $-1$ to $\{1, 0\}$. '1' implies transmitted pulse and '0' implies omitted pulse. In the corresponding reference sequence of the Barker-based waveform $+1$ is converted to $\{-1, 1\}$ and $-1$ is converted to $\{1, -1\}$. The reference sequence is implemented numerically in the receiver, hence can take any value. Rows 2 and 3 of Table 2 list one period (8 PRIs in a period, PRI $= T_r$) of the transmitted pulses and the reference sequence of Barker 4-based signal. Fig. 1 displays five transmitted code periods (top) and two reference periods (bottom). Omitted pulses in the transmitted train appear as negative pulses in the reference sequence. This mismatched filter produces cross-correlation (Fig. 2) that differs from ideal periodic response only by two negative side lobes (SL) at $\pm T_r$ around the periodic main lobe. The negative SL level is half that of the main lobe. The response periodicity is 8 PRIs, implying extension of the unambiguous range by a factor of 8. In reality, the periodic transmission continues indefinitely and the reference length is set according to the TOT of the rotating antenna.

The receiver performs envelope detection; hence, the detected pulses are positive, like the transmitted pulses. The response displayed to the user contains only the positive values in Fig. 2. To perform conventional non-coherent integration, the reference sequence is as listed in the bottom row of Table 2, which is identical to the transmitted PRI-coded pulse train. This means performing cross-correlation with a matched signal. The resulted output will consist of all the correlation lobes, equally spaced by $T_r$. However,

**Table 1** Parameters of Furuno 1623 civil marine radar

| Displayed range, nm | Pulse-width, μs | PRF (=1/PRI), Hz | Antenna rotation speed, rpm |
|---|---|---|---|
| 0.75 | 0.08 | 3000 | 41 |
| 16 | 0.8 | 600 | 24 |

**Table 2** Transmitted and reference pulses based on Barker 4 coding

| Pulse # | 1 | 2 | 3 | 4 | 5 | 6 | 7 | 8 |
|---|---|---|---|---|---|---|---|---|
| Trans. | 0 | 1 | 1 | 0 | 1 | 0 | 1 | 0 |
| Ref. 1 | −1 | 1 | 1 | −1 | 1 | −1 | 1 | −1 |
| Ref. 2 | −0.5 | 1.5 | 0.5 | −0.5 | 0.5 | −0.5 | 0.5 | −1.5 |
| Ref. 3 | −0.75 | 1.25 | 0.75 | −0.75 | 0.75 | −0.75 | 0.75 | −1.25 |
| Ref. NC | 0 | 1 | 1 | 0 | 1 | 0 | 1 | 0 |

their heights will vary because of the coding. The two kinds of responses will be demonstrated in the experimental results.

The pulse train generated by Manchester-coded Ipatov 5 and the corresponding reference pulses are listed in rows 2 and 3 of Table 3. Note that the reference pulses utilise two magnitudes. This fact poses no difficulty because the reference pulses are numerical values in the receiver's processor. The delay response in the Ipatov-based signal is similar to Fig. 2, except for the periodicity which becomes 10 $T_r$.

Clearly, there are two requirements from the code on which the transmitted waveform is based: (a) it must be binary, to allow Manchester coding; (b) it should exhibit ideal periodic autocorrelation (which Barker 4 is the only one that does) or low-loss, ideal, periodic cross-correlation (which Ipatov 5 exhibits). Although there are no more binary codes with ideal periodic autocorrelation, there are more and longer, Ipatov codes. After Ipatov 5 the next one is Ipatov 13. This, and longer lengths are, however, of little use for marine radar application. There is no practical value

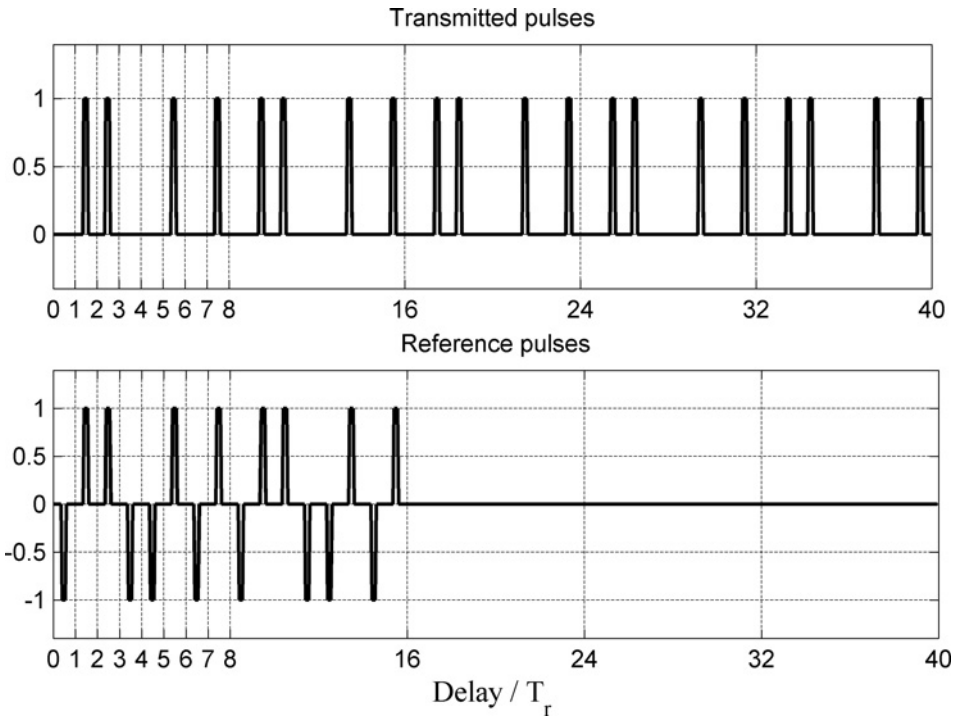


**Fig. 1** *Transmitted and reference pulse trains based on Manchester-coded Barker 4 sequence*

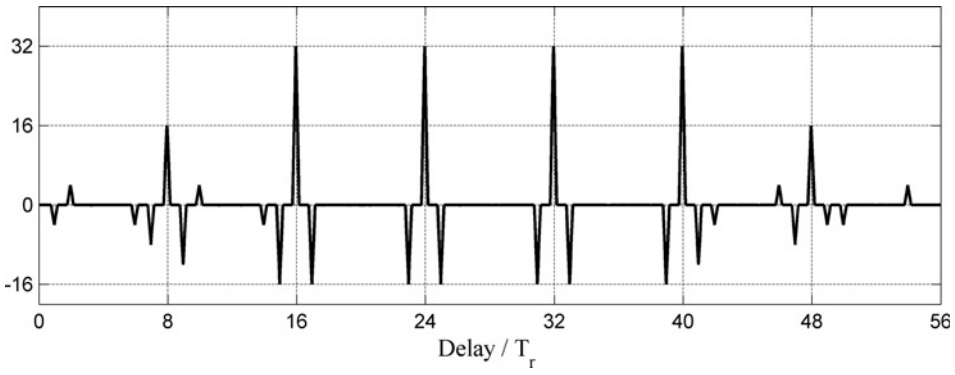


**Fig. 2** *Cross-correlation of the transmitted and reference pulse trains in Fig. 1*

**Table 3** Transmitted and reference pulses based on Ipatov 5 coding

| Pulse # | 1 | 2 | 3 | 4 | 5 | 6 | 7 | 8 | 9 | 10 |
|---|---|---|---|---|---|---|---|---|---|---|
| Trans. | 1 | 0 | 1 | 0 | 1 | 0 | 0 | 1 | 1 | 0 |
| Ref. 1 | 1 | −1 | 1 | −1 | 1 | −1 | −2 | 2 | 1 | −1 |
| Ref. 2 | 0.5 | −0.5 | 0.5 | −0.5 | 0.5 | −2 | −1 | 2.5 | 0.5 | −0.5 |
| Ref. 3 | 0.75 | −0.75 | 0.75 | −0.75 | 0.75 | −1.75 | −1.25 | 2.25 | 0.75 | −0.75 |
| Ref. NC | 1 | 0 | 1 | 0 | 1 | 0 | 0 | 1 | 1 | 0 |

to extend the unambiguous range from a factor of 10, which Ipatov 5 provides, to a factor of 26, which Ipatov 13 can provide. For the same target the received power from 10 times the range will be weaker by a factor of 10 000; but from 26 times the range it will be weaker by a factor of 457 000. In conclusion, waveforms based on Barker 4 or Ipatov 5 are the only relevant ones. The story is different with regard to the reference waveforms used in the correlation receiver. How to design them is discussed next.

## 3 Modified references

The main drawback of the delay response in the top subplot of Fig. 3 is the strong negative side lobe at $\tau = T_r$. It implies that the strong direct reception of the transmitted pulse, followed by strong returns from near-clutter, will appear at and immediately after $\tau = 0$ but will also create a corresponding deep null ('hole') at and immediately following $\tau = T_r$. The depth of the 'hole' is half the height of the direct reception and the near-clutter. True targets near that delay are likely to be concealed, creating an effective 'blind range'. There is therefore a motivation to push that 'hole' farther away and make it shallower. Ref. 2 (4th row of Table 2) achieves that. Under ideal conditions, in which all the transmitted pulses have identical amplitude, the response attained with Ref. 2 will be optimal. It is shown in the middle subplot of Fig. 3. Ref. 2 ($R_2$) is obtained from Ref. 1 ($R_1$) using the relationship

$$R_2(n) = R_1(n) + 0.5R_1(n+1) \tag{1}$$

In practice, the transmitted pulses are not identical. For example, when the PRI is reduced considerably below its original value, the magnetron pulses tend to change amplitude in some relation to the pause they follow. When the transmitted pulses are not identical the response obtained with the three references listed in Table 2 may look like the plots in Fig. 4.

The positive sidelobe at delay = PRI (marked by the arrow) is the most bothersome. It causes the direct reception and near-clutter to reappear as positive side lobes around that delay. Even when attenuated by 50 or 60 dB, they still are of similar intensity to expected true targets at that delay. That issue prompted the use of Ref. 3 (see Table 2). The ideal response of Ref. 3 exhibits two shallow negative holes at PRI and 2*PRI (see Fig. 3, lower subplot). Those side lobes are expected to remain negative (Fig. 4, lower subplot) despite intensity fluctuations of the transmitted pulses. Ref. 3 ($R_3$) is obtained from Ref. 1 ($R_1$) using the

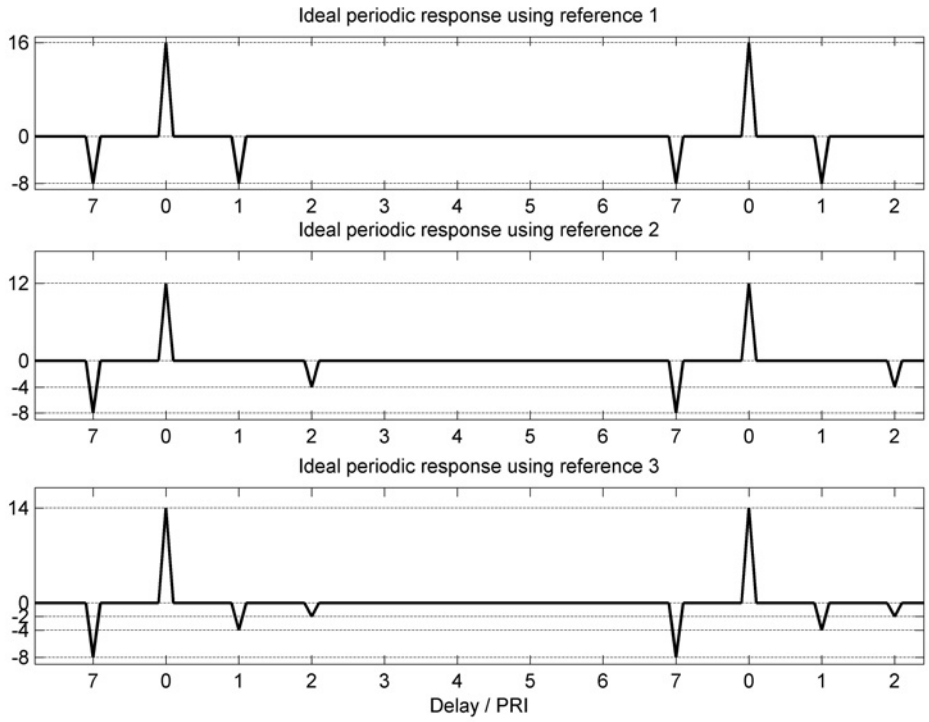


**Fig. 3** *Three responses obtained with the three references listed in Table 2 (identical transmitted pulses)*




doi: 10.1049/iet-rsn.2011.0372

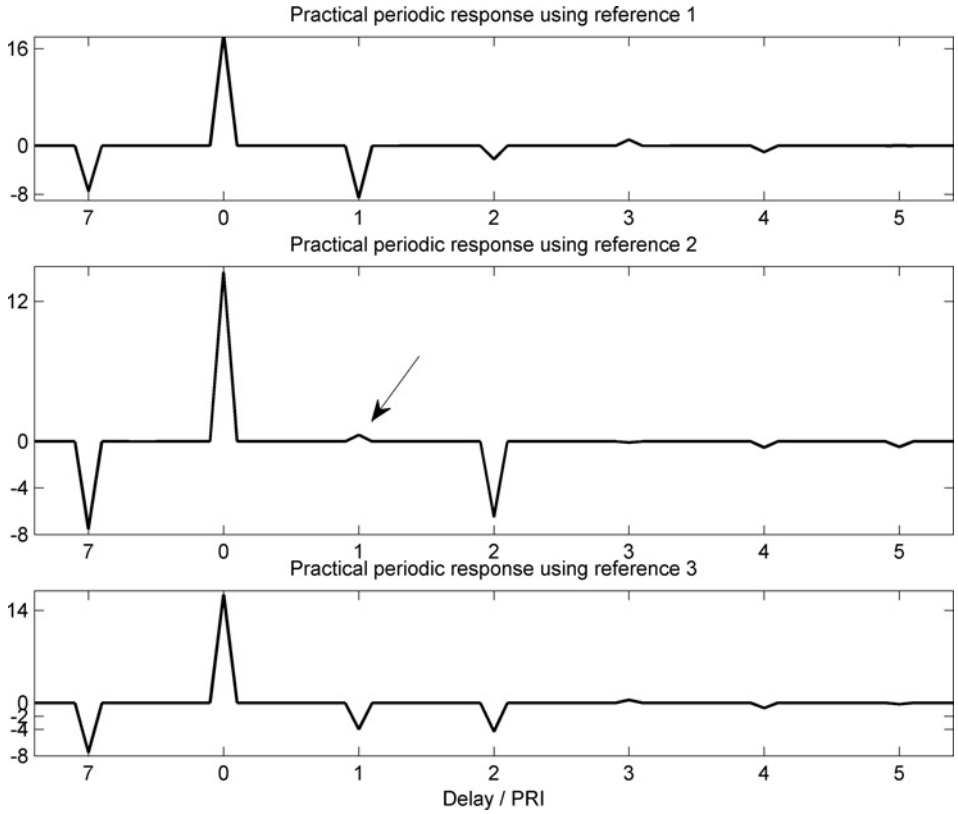


**Fig. 4** *Three responses obtained with the three references in Table 2 (fluctuating transmitted pulses)*

relationship

$$R_3(n) = R_1(n) + 0.25R_1(n+1) \tag{2}$$

The factor 0.25, which multiplies the shifted original reference sequence, was found experimentally to be a safe value that will not allow a positive sidelobe at $\tau = T_r$, with the kind of transmitted pulse fluctuations in our specific field trial.

## 4 Detection statistics

The main property of the PRI coding is an extension of the unambiguous range. However, there is another benefit to the inherent mismatch between transmitted and reference waveforms. As Ref. 1 in Tables 2 and 3 are balanced (as are Refs. 2 and 3), integration and detection of noise background are expected to exhibit probability density function (PDF) with zero mean. With many integrated pulses, the PDF approaches zero-mean Gaussian shape. The PDF of conventional non-coherent integration is well known, and in the case of many integrated pulses it approaches a Gaussian PDF with non-zero mean. Simulation results exhibited the expected PDFs in Figs. 11, 12 and 13 of [2]. An example of the detectors outputs, obtained from a preliminary field trial (Tel-Baruch, 30 November 2010), is shown in Fig. 5. They show detector

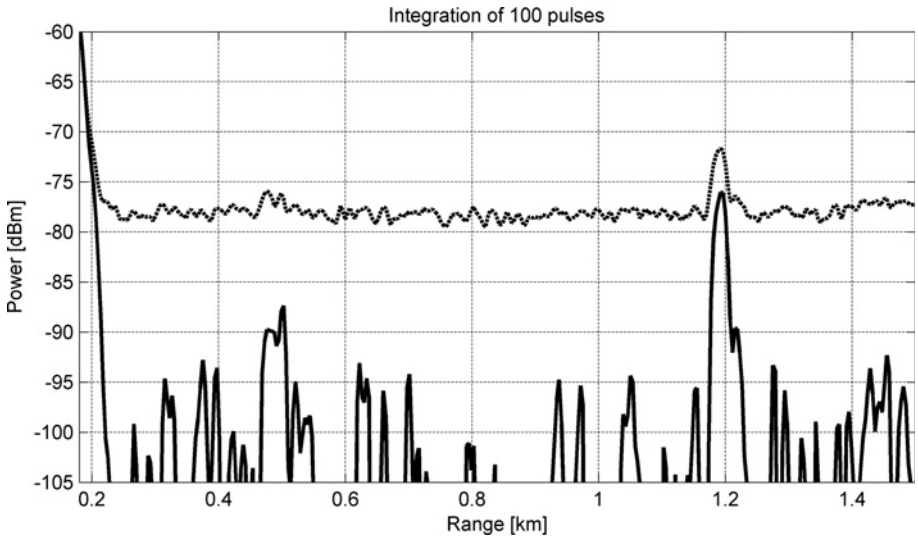


**Fig. 5** *Detector output using conventional non-coherent integration (dash) and Ipatov processing (solid)*

output from a calm sea scene with a small boat at 1.2 km. The transmitted PRI was coded according to Ipatov 5 sequence (Table 3, row 2). The reference for the conventional non-coherent integration of 100 pulses follows 20 sequences of Ref. NC (Table 3, row 6), and yielded the dash line. The reference for the Ipatov processing follows 20 sequences of Ref. 1 (Table 3, row 3), and yielded the solid line. The expectation that Ipatov/Barker processing output, when detecting noise, will be centred on zero value is confirmed by the solid line plot (only positive values were used before converting to logarithmic scale). The mean of the conventional non-coherent integration of noise (around −78 dBm) hints that setting an adaptive threshold for constant false alarm ratio (CFAR) will require estimation of two parameters (mean and variance), whereas for Ipatov/Barker processing only the variance needs to be estimated.

It is interesting to note that J.I. Marcum, in his seminal 1947 research memorandum [4], suggested a scheme for non-coherent integration '… in which a pulse known to be only noise is subtracted from each possible signal plus noise pulse. $N$ of these composite pulses are then integrated. With no signal, the average value of any number of such composite pulses is nearly zero …'.

The '(signal + noise) − noise' integration scheme uses a mismatched reference, and some signal-to-noise ratio (SNR) loss is expected. In the appendix to his research memorandum (following Eq. 184), Marcum states that 'There appears to be no significant difference in the probabilities of detection for N between 1 and 10 (pulses). For N between 100 and 1000, the composite case gives an effective signal-to-noise ratio about 1 dB lower than the ordinary case'. Detection simulations described in Table 4 of [2] show an SNR loss of 1.25 dB, when 60 non-fluctuating pulse returns are integrated to achieve $P_{FA} = 0.001$, $P_D = 0.95$. The field trials, described next, indeed do not show clear difference in detection probabilities between the two non-coherent integration schemes. We do not know if and where Marcum's alternative integration scheme was implemented. With our waveform it is an inherent by-product.

## 5 Field trial results

The field trials were conducted with a Furuno 1623 low-cost, magnetron-based, civil marine radar. The radar was modified to provide control of pulse triggering and to extract the IF output. Our circuitry performed analog-to-digital conversion of the IF output, and all the processing was digital from that point on. The radar operates at X-band (9.41 GHz). It has a 15′ antenna, providing 6.2 degree horizontal beam-width. The peak pulse power is 2.2 kW. We mainly used the narrow pulses (0.08 μs). At that PW the antenna rotation rate is 41 rpm. Thus, a point target is illuminated for 25 ms every 1.46 s. At a nominal PRF of 6250 Hz, the 8 pulse positions in a Barker-coded period occupy 1.28 ms, namely, the target illumination contains approximately 19 Barker-code periods or 72 transmitted pulses. This is therefore the length of the reference sequence. Hamming-weight amplitude-multiplies the reference sequence. Two hundred and forty pulses are integrated when the highest (20 kHz) PRF is used.

The main purposes of the field trial were: (a) to test the extension of the unambiguous range by the proposed coding (Barker and Ipatov); (b) to demonstrate the improved resolution of using short pulses. To be able to see targets beyond the un-coded unambiguous range (=C/PRF/2) we needed distant large ships. The required scene is available near the port of Ashdod. The radar was mounted on a tripod placed on a small dune in the southern most beach of the city of Ashdod. The port of Ashdod and the area of waiting ships were to the north and north-west. We also detected ships waiting to unload fuel for the power station in Ashkelon at the south.

As half the pulses are not transmitted, it is hardware-safe to raise the PRF beyond its original highest value. Instead of using the nominal highest PRF of 3 kHz, we raised the PRF to values between 6 and 20 kHz. The results shown in this paper were taken with PW of 80 ns and PRF of 12.5 kHz. They are compared to the un-coded case of PW of 800 ns and PRF of 625 Hz. Without coding, PRF = 12.5 kHz implies an unambiguous range of 12 km. With coding, as in Tables 2 and 3, the corresponding unambiguous ranges become 96 km (Barker) and 120 km (Ipatov).

Figs. 6 and 7, obtained from the same single antenna sweep, provide comparison between conventional non-coherent integration (using Ref. NC, Table 3) and Ipatov

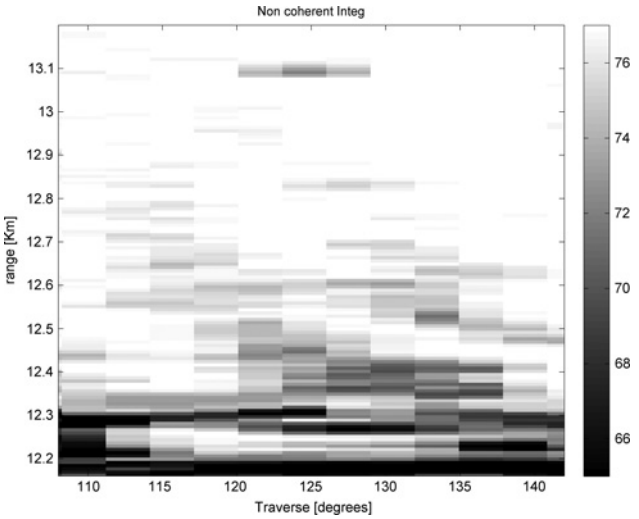


**Fig. 6** *Ship at 13.1 km among replicated near-clutter*
Non-coherent integration. PW = 80 ns, PRF = 12.5 kHz

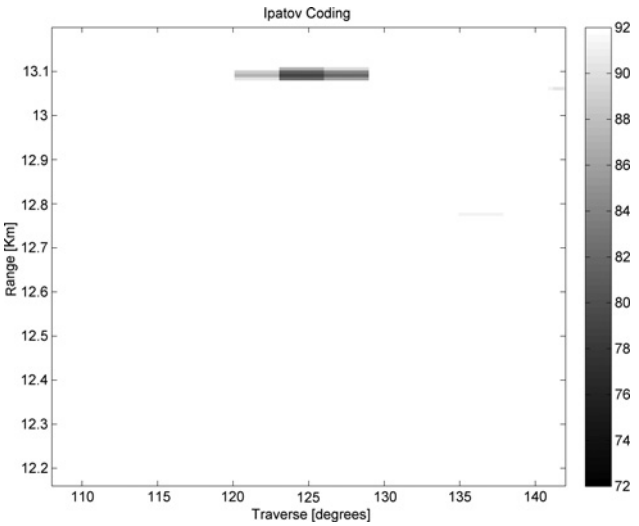


**Fig. 7** *Ship at 13.1 km in the clear*
Ipatov processing. PW = 80 ns, PRF = 12.5 kHz




doi: 10.1049/iet-rsn.2011.0372

processing (using Ref. 3, Table 3). The detected target is a ship at 13.1 km facing Ashkelon. The graybar is in negative dB. With PRF = 12.5 kHz the unambiguous range is 12 km. Indeed in Fig. 6 the near-clutter replicates at and beyond that range, making it difficult not to confuse the ship with replicated near-clutter. Owing to the Ipatov processing, in Fig. 7 the ship is in the clear. Where the near clutter was seen before there is now a 'hole'. The 'hole' at 12 km is made visible in Fig. 8 by extending the dynamic range and reversing the sign of the graybar.

Fig. 9 demonstrates the improved range resolution obtained with the narrow pulse (PW = 80 ns, PRF = 12.5 kHz). It displays a cluster of ships facing the port of Ashdod. The transmitted sequence was Barker-coded (Table 2). Fig. 9 displays the result of processing a single antenna sweep, using Ref. 3. The same returns were also processed using Ref. NC, yielding very similar detection results (up to 12 km).

The pixel range width is 7.5 m, smaller than the range resolution (12 m) of an 80 ns pulse. The traverse pixel width is 3°, half the antenna beam-width. 3° convert to about 300 m at a range of 5.7 km. Observing the two nearest targets Fig. 9 suggests that the ship at 5.7 km is aligned approximately along the radial direction, whereas the ship at 5.4 km is aligned approximately cross-range. The zoom in Fig. 10 details the range profile of the ship at

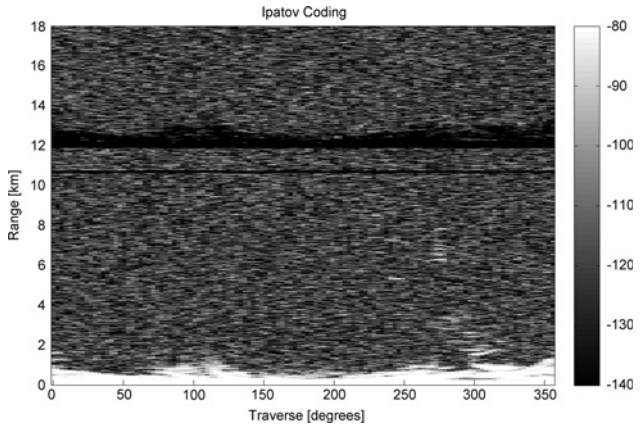


**Fig. 8** *'Hole' at 12 km. Ipatov processing*
PW = 80 ns, PRF = 12.5 kHz. (The additional narrow 'hole' at 10.8 km resulted from a hardware flaw)

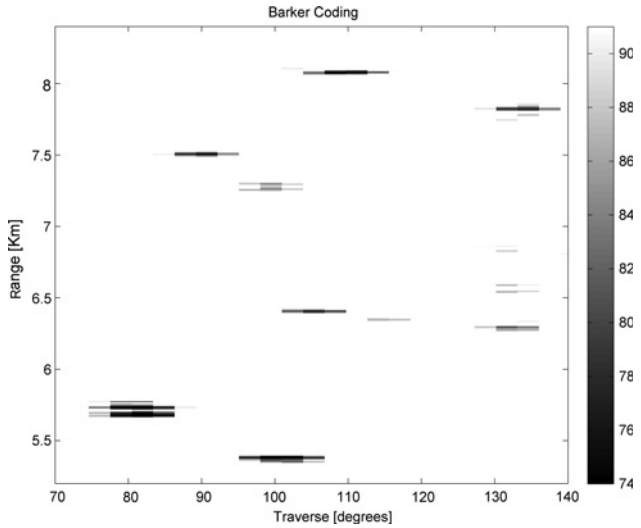


**Fig. 9** *Ships facing Ashdod. Barker processing*
PW = 80 ns, PRF = 12.5 kHz

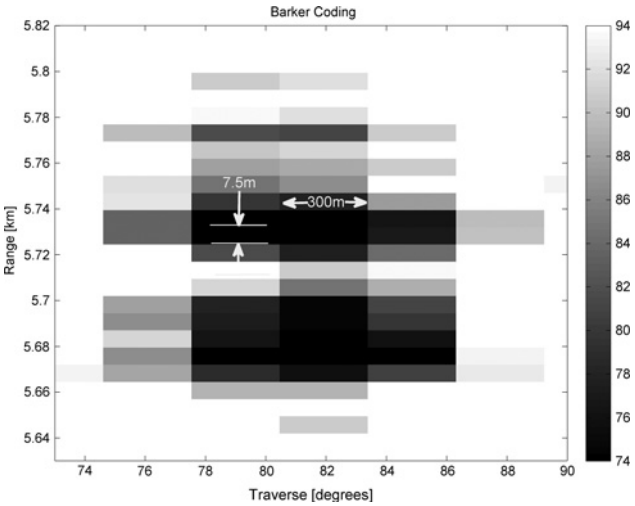


**Fig. 10** *Zoom on the ship at 5.7 km*
Barker processing. PW = 80 ns, PRF = 12.5 kHz

**Fig. 11** *Ship whose radar profile appears in Fig. 10*

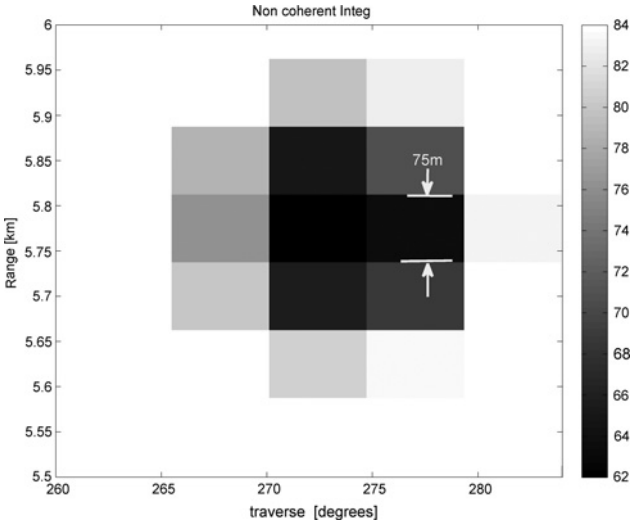


**Fig. 12** *Zoom on the ship at 5.7 km*
Non-coherent integration, PW = 800 ns, PRF = 625 Hz

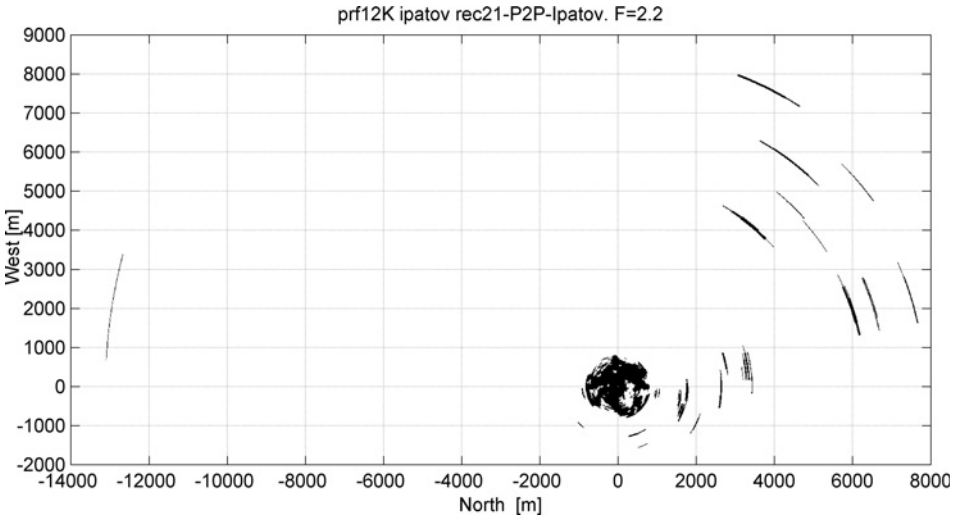


**Fig. 13** *Radar scene after Ipatov integration, along-range CFAR, and 2-out-of-10 binary integration*

5.7 km. It suggests the ships total range span of 150 m, divided into three or four along-range scattering zones. This profile is supported by the photograph in Fig. 11. The cross-range dimension of the ship cannot be estimated because of the poor azimuth resolution.

In order to demonstrate how much the range resolution was improved by the narrow pulse, Fig. 12 shows the same ship as in Figs. 10 and 11 (taken several hours apart) with the radar in its original mode (PW = 800 ns, PRF = 625 Hz, rotation speed = 24 rpm). Note that the traverse scale is randomly offset from one run to another, and that the traverse pixel width in this mode is about 5°. With range resolution of 120 m and pixel range width of 75 m, little or no information on aspect and radial dimensions can be deduced.

Another important advantage of using an 80 ns pulse rather than 800 ns is the reduced clutter illumination area by a factor of 10. Regrettably, during our field trials the sea was relatively calm, and this advantage could not be demonstrated.

The entire radar scene is displayed in Fig. 13. It was obtained from Ipatov processing (PW = 80 ns, PRF = 12.5 kHz) during ten consecutive antenna scans. In each scan, an along-range CFAR was performed every 3°. Binary integration (two out of ten) followed the ten antenna scans. The resulted binary map was then converted to range–range coordinates. The radar is located at (0, 0). The ship target facing Ashkelon appears at (−13 000, 2000). The ships cluster facing Ashdod is seen around (5000, 5000).

## 6 Interference mitigation

Taking over all the receiver operations after the IF amplifier meant losing some built-in features of the original radar. We did not try to reproduce all the features and controls in order to create a fully operational product. However one issue needed attention and that was interference from marine radar on other ships. The quick *ad-hoc* fix to this kind of interference was to repeatedly arrange the sampled detection in a numerical array in which each row contained the detected samples from one coded period (e.g. from 10 nominal PRIs, in the Ipatov case), and the number of rows was equal to the number of code sequences to be integrated later (e.g. 20 rows, when integrating returns from 100 transmitted pulses). Thus each column represents a range bin. On each column we removed any detection which is 10 dB over the 60th percentile of all the elements in that column, and replaced it with its neighbours. Once those outliers were removed, the integration (= correlation) was performed.

## 7 Summary and discussion

Our experimental results show the feasibility of extending the unambiguous range of magnetron pulse radar. On transmit, half of the pulses are eliminated according to a periodic code. On receive, the pulses are envelope detected and then cross-correlated with numerically implemented reference pulses that use two polarities and variable amplitudes. This concept allows operating the radar in a ‘short pulse, short PRI’ mode even at long-range settings. That mode maintains the average transmitted power, improves the range resolution and reduces clutter illumination. Being able to use narrow pulses is especially important in magnetron radar, where there is no option to perform pulse-compression. The experiment was performed using modified low-cost 2.2 kW magnetron radar (Furuno 1623). Eighty ns pulses were transmitted at PRFs as high as 20 kHz.

The main penalties of the demonstrated approach are blind ranges (‘holes’ in the response), at delays equal to the PRI and its multiples. The hole’s width equals the width of the strong near-clutter. In our experiment, with the radar on shore, that width was approximately 300 m. In case of radar at sea the strong near-clutter is expected to be narrower, resulting reduced chance of concealed targets.

The blind range difficulty can be mitigated by switching, once per antenna revolution, between two slightly different PRIs. Detection decisions based on binary integration of two antenna scans, with a binary integration rule of ‘at least one-out-of-two’, is likely to reveal all detectable targets. The combination of the small chance of having a target in the blind range, and the high effectiveness of the binary integration, promise this to be a good fix.

The special form of the reference signal implements Marcum’s alternative non-coherent detection scheme ‘(signal plus noise) minus noise’. The small SNR loss (∼1 dB), predicted by Marcum and by our own simulations, was indeed observed in the field trial. Up to the original unambiguous range, both detection schemes yielded similar detection probabilities. Also, the zero




doi: 10.1049/iet-rsn.2011.0372

average output when detecting noise with that scheme was helpful in threshold setting.

## 8 Acknowledgment

This work was supported by the chief scientist of the Israel Ministry of Industry, Trade and Labor. We thank the chief scientist and the technical referee Mr. S. Gabbay.

## 9 References

1 Briggs, J.N.: 'Target detection by marine radar' (IEE, 2004)
2 Levanon, N.: 'New waveform design for magnetron-based marine radar', *IET Radar Sonar Navig.*, 2009, **3**, (5), pp. 530–540
3 Levanon, N., Mozeson, E.: 'Radar signals' (Wiley, Hoboken, NJ, 2004), Sec. 6.5
4 Marcum, J.I.: 'A statistical theory of target detection by pulsed radar', RAND Corp. Res. Mem. RM-754, 1 December 1947 (Reprinted in the *IRE Trans. Inf. Theory*, 1960, **6**, (2), pp. 59–267)